Computational Modelling of Concrete and Concrete Structures – Meschke, Pichler & Rots (Eds)

On the modelling of the rate dependence of strength using a crack-band based damage model for concrete

X. Liu, C.H. Lee & P. Grassl
James Watt School of Engineering, University of Glasgow, Scotland, UK

ABSTRACT: Concrete strength is reported in literature to increase with increasing strain rate, which needs to be considered in concrete constitutive models used for finite element analyses of concrete structures. One attractive group of constitutive models for concrete failure are scalar damage models using the crack band approach. These models are computationally efficient for rate independent loading because they produce mesh independent results with coarse discretisations as long as the strain field localises in mesh-dependent zones. The aim of this study is to incorporate the strain rate dependence in crack band based damage models while maintaining their ability to produce mesh-independent results. First the proposed model is described. Then, it used for direct tensile analysis in which strain softening occurs. It is demonstrated that a combination of strain rate dependent model for the undamaged response combined with a relative displacement rate dependent model for the damaged response provides stress-displacement curves which converge with mesh refinement.

1 INTRODUCTION

Critical infrastructure made of reinforced concrete are required to be designed to resist fast dynamic loading in the form of impact, sudden ground acceleration and blast, which can arise due to collisions, earthquakes and explosions, respectively. Concrete structures subjected to dynamic loading exhibit a complex nonlinear failure response which differs significantly from the one due to quasi-static loading. For instance, structures subjected to impact and blast can exhibit localised shear failure for loads, which, if they were applied slowly, would result in bending failure. Furthermore, dynamic loading produces compressive shock waves which can cause tensile spalling of the concrete cover, if reflected at free boundaries. Fast dynamic loading produces higher stiffness and strength than quasi-static loading. Strength of concrete is reported in the literature to be significantly increased for high strain rates (Bischoff & Perry 1991; Malvar & Ross 1998), whereas for fracture energy the results are less conclusive (Doormaal et al. 1994; de Pedraza et al. 2018).

For finite element modelling of failure of concrete structures, constitutive models for concrete are required, which can model localised tensile and diffuse compressive fracture. Approaches suitable for this are regularised continuum approaches which describe tensile fracture by means of mesh-independent zones of localised strains. One group of these regularised models for dynamic loading are based on the concept of damage delay (Häussler-Combe and Kühn 2012; Piani et al. 2019). One of the limitations of these approaches is that a very fine mesh is needed so that the zones of localised strain are modelled mesh-independently. Therefore, this approach less suitable for modelling structural components of reinforced concrete. Alternatively, discrete element approaches, in the form of lattice or particle models are used to model fracture in concrete. In these approaches, rate dependence of strength is modelled by cohesive laws which depend on the rate of the crack opening (Cusatis 2011). The third group of constitutive models are hybrid approaches in which the continuum and discrete models are combined. One numerically efficient hybrid approach are crack band models (Bažant & Oh 1983; Pietruszczak & Mróz 1981; Willam et al. 1986). In these approaches, cracks are described by using strain softening, which results in mesh-dependent localised zones. Mesh dependence of load displacement curves is avoided by adjusting the softening part with respect to the element size. These crack band models are popular choice for concrete, because they produce mesh-independent results for coarse discretisations. Therefore, they can be used for analysing the failure response of reinforced concrete components. The challenge for formulating crack band approaches for dynamic loading as a function of the strain rate is that the strain profiles obtained are mesh-dependent. As a consequence, the strain rate in the localised zones are also mesh-dependent. As the mesh is refined, the strain rate in the localised zones increases, which results in an artificial strengthening of the material.

DOI 10.1201/9781003316404-61

The aim of the present study is to propose a technique to provide mesh-independent load-displacement curve for strain rate dependent material responses used within the crack band approach. We use a scalar damage model to the illustrate the modelling concept. However, crack band models can be applied to a range of constitutive models, such as plasticity and damage-plasticity models (Grassl et al. 2013). The first part of the paper is used to introduce the rate dependent damage model. This is done in three steps. First, the standard rate independent model is presented. Next, the approach in which the damage evolution is made a function of the strain rate. Finally, the newly proposed formulation which produces mesh-independent results is presented. All three approaches are applied to an one-dimensional bar subjected to uniaxial tension to illustrate the differences of the formulations.

2 SCALAR DAMAGE MODEL

The approach to model the rate dependence of concrete is demonstrated here by a scalar damage model. First, the standard rate independent model is presented. This is followed by a description of the extension of the model that is modified to take into account rate dependence.

2.1 Rate independent model

The constitutive model used here is a strain based damage model for which the nominal stress $\boldsymbol{\sigma}$ is

$$\boldsymbol{\sigma} = (1-\omega)\,\bar{\boldsymbol{\sigma}} = (1-\omega)\,\mathbf{D}_\mathrm{e} : \boldsymbol{\varepsilon} \tag{1}$$

where $\mathbf{D}_\mathrm{e}$ is the elastic stiffness based on the Young's modulus E and Poisson's ratio ν, $\bar{\boldsymbol{\sigma}}$ is the effective stress, tensor $\boldsymbol{\varepsilon}$ is the strain tensor and ω is the damage variable ranging from 0 (undamaged) to 1 (fully damaged).

The damage variable ω is determined from a history variable κ. The history variable κ is obtained by a damage loading function of the form

$$f = \tilde{\varepsilon} - \kappa \tag{2}$$

with the loading and unloading conditions

$$f \leq 0 \;\; \dot{\kappa} > 0 \;\; \dot{\kappa} f = 0 \tag{3}$$

Here, the equivalent strain $\tilde{\varepsilon}$ is

$$\tilde{\varepsilon} = \frac{1}{E}\sqrt{\sum_{I=1}^{3} \langle \bar{\sigma}_\mathrm{I} \rangle^2} \tag{4}$$

where $\bar{\sigma}_\mathrm{I}$ are the principal values of the effective stress and $\langle \bar{\sigma}_\mathrm{I} \rangle$ are their positive parts. This equivalent strain definition gives a modified Rankine strength envelope at the onset of damage as shown in Figure 1. For $\tilde{\varepsilon} > f_\mathrm{t}/E$, damage occurs. The evolution of the damage variable is formulated so that in uniaxial tension

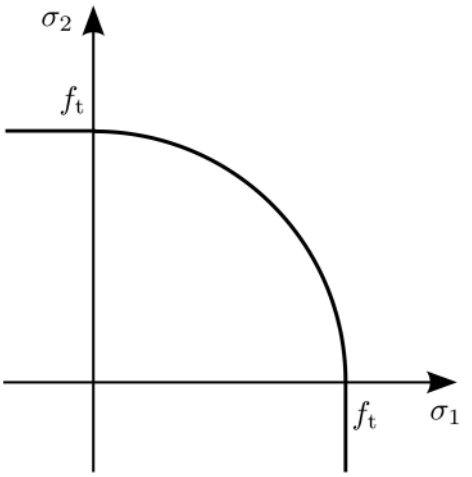

Figure 1. Strength envelope.

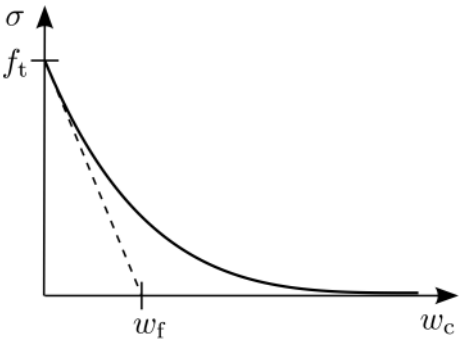

Figure 2. Stress crack-opening curve in uniaxial tension.

an exponential stress-crack opening curve as shown in Figure 2 is obtained. This is achieved by solving

$$(1-\omega)\,E\kappa = f_\mathrm{t} \exp\left(-\omega \kappa h_\mathrm{e}/w_f\right) \tag{5}$$

for ω using the standard Newton-Raphson method. Here, h_e is the characteristic element length, f_t represents the tensile strength and w_f is the crack opening threshold in Figure 2. The left hand side of (5) is equal to the expression for $\boldsymbol{\sigma}$ in (1) for the case of monotonic uniaxial tension with the uniaxial strain replaced by κ. The right hand side shows the exponential softening law (Figure 2) whereby the crack opening is expressed by $\omega \kappa h_\mathrm{e}$.

2.2 Extension to strain rate dependence

The scalar damage model presented in the previous section is for quasi-static loading in which the strength is independent of the strain rate. The main purpose of this work is to introduce a modification of the damage model so that strain rate dependence of strength can be taken into account in the constitutive model. One approach would be to delay the evolution of the equivalent strain so that damage is initiated at a higher stress.

This can be achieved by reformulating expression (5) to be

$$(1-\omega)\,E\kappa_1 = f_t \exp\left(-\omega\kappa_2 h_e / w_f\right) \tag{6}$$

where κ_1 and κ_2 are determined in rate form as

$$\dot{\kappa}_1 = \dot{\kappa}/\alpha \text{ and } \dot{\kappa}_2 = \dot{\kappa}\alpha \tag{7}$$

Here, α is a (scalar) strain rate dependent factor, which, in this work, is based on *fib* Model Code (CEB-FIP 2012). It has the form

$$\alpha = \begin{cases} 1 & \text{for } \dot{\tilde{\varepsilon}} \le \dot{\varepsilon}_1 \\ \left(\dfrac{\dot{\tilde{\varepsilon}}}{\dot{\varepsilon}_1}\right)^{0.018} & \text{for } \dot{\varepsilon}_1 \le \dot{\tilde{\varepsilon}} \le \dot{\varepsilon}_2 \\ 0.0062\left(\dfrac{\dot{\tilde{\varepsilon}}}{\dot{\varepsilon}_1}\right)^{1/3} & \text{for } \dot{\varepsilon}_2 \le \dot{\tilde{\varepsilon}} \end{cases} \tag{8}$$

where $\dot{\varepsilon}_1 = 1 \times 10^{-6}$ s^{-1} and $\dot{\varepsilon}_2 = 10$ s^{-1}. It should be noted that the specific expression of α is not important for this study, since it is not aimed to reproduce experimental results, but to propose a formulation that is mesh-independent. Comparing expression (6) with (5), the term κ on the left hand side of (6) is replaced by κ_1 so that for strain rates which result in $\alpha > 1$, the stress at which damage starts is greater than the tensile strength. Keeping the same spirit, the term κ_2 is used on the right hand side of (6) for the crack opening in order to ensure that the fracture energy remains constant with increasing strain rate. Both κ_1 and κ_2 are given in rate form as described in (7).

The problem with this formulation is that the rate factor α is a function of the strain rate, which for the crack band model is mesh-dependent once damage is initiated. Therefore, finer meshes will produce greater rate factors and therefore, higher strengths. To overcome this mesh dependence, the rate factor α is made a function of the displacement rate once damage is induced. To achieve a continuous evolution of the rate factor for the transition from undamaged to damage state, the strain rate before the onset of damage is linked to the displacement rate after the onset of damage by means of the incremental form

$$\frac{\tilde{\varepsilon}^n - \tilde{\varepsilon}^{n-1}}{t^n - t^{n-1}} = \beta h_e \frac{\tilde{\varepsilon}^{n+1} - \tilde{\varepsilon}^n}{t^{n+1} - t^n} \tag{9}$$

where $n+1$ is the first step where damage is nonzero. The parameter β is determined once at the start of damage and then kept constant. The material models described above were implemented in the open source finite element program OOFEM (Patzák 2012).

3 MESH DEPENDENCE STUDY

The response of the three crack band damage models above, namely rate-independent, strain-rate dependent and displacement rate dependent is investigated for possible mesh-dependence by means of a direct tensile analysis. For being able to investigate the material response independent of wave propagation, the problem is solved assuming zero mass for the material. Consequently, the results presented here are based on force equilibrium only without the inertia term. The geometry of the bar is shown in Figure 3. One element in the centre of the bar is strongly weakened to trigger the onset of failure. The length of the bar is $L = 0.1$ m and the cross-sectional area is $A = 0.01$ m^2. Four meshes with 1, 5, 10 and 20 equally sized elements are used. For the weakened element, the properties are $f_t = 3$ MPa, Young's modulus $E = 30$ GPa and fracture energy $G_F = 100$ N/m. The adjacent elements have the same Young's modulus, but a much higher strength of 15 MPa so that damage is limited to the weakened element for all the analyses. The analysis is displacement controlled at the end of the specimen with a displacement rate of 5 m/s. For the elastic stage during which the strain is uniformly distributed, this corresponds to a strain rate of 50 1/s and rate factor of $\alpha = 2.28$ according to (8). The first set of analyses were carried out with the strain-rate independent model. The load displacement curve and strain profiles are shown in Figures 4 and 5, respectively. The load-displacement curves are mesh-independent. However, the strain profiles depend on the number of elements. This is a typical result for crack band models with rate independent material models in which the cracks are represented by mesh-dependent zones of high strain values. In the present setup, the high strain occurs in the weakened element, whereas in the other elements unloading occurs. For quasi-static simulation,

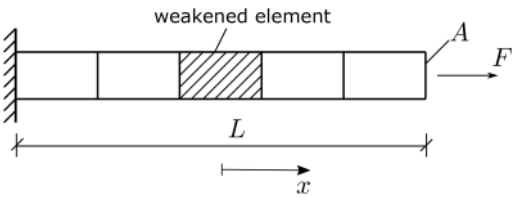

Figure 3. Geometry of specimen for mesh dependence study.

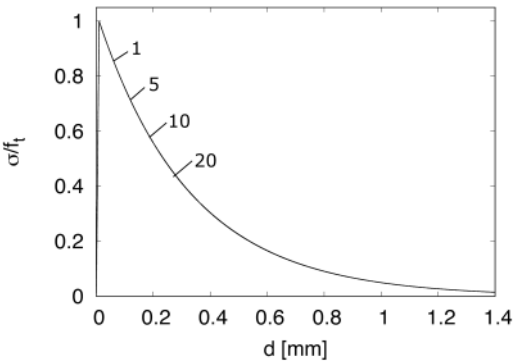

Figure 4. Normalised stress versus displacement for four meshes for the rate independent damage model.

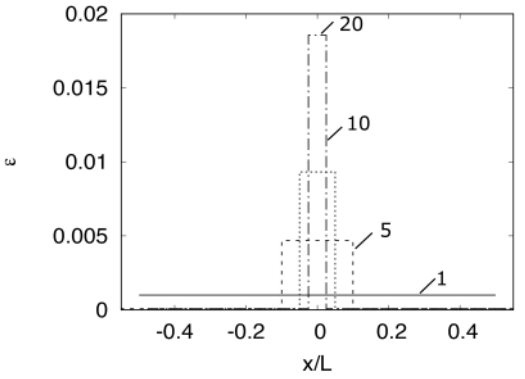

Figure 5. Strain versus x-coordinate for four meshes for the rate independent damage model at a displacement of 0.1 mm.

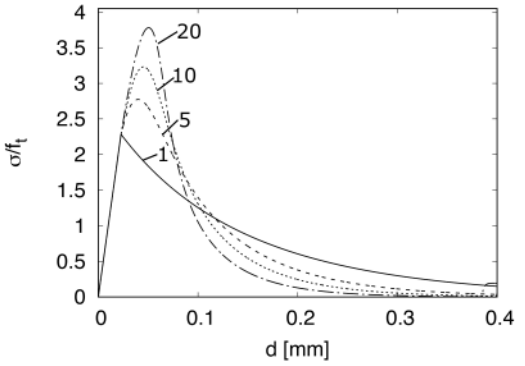

Figure 6. Normalised stress versus displacement for four meshes for the strain rate dependent damage model.

the mesh-dependent zones are not problematic, since in general the main aim is to obtain mesh-independent load-displacement curves. However, this is not the case for strain rate dependent models as the mesh-dependence of the strain causes problems which will be illustrated in the next part.

In the second part, the results for the strain rate dependent scalar damage model are presented. In Figures 6 and 7, the load-displacement and rate factor are shown, respectively. The load-displacement response in Figure 6 and the rate factor in Figure 7 are strongly mesh-dependent. The finer the mesh is, the greater is maximum peak load and rate factor. This mesh-dependence of the load-displacement response and rate factor is explained by Figure 5. The strain localises in mesh-dependent region. Therefore, for the same displacement, the strain and also strain rate in smaller zones is greater. Therefore, the finer the mesh, the greater is the strain rate and the rate factor. Note that an increase in the rate factor does not result in a jump in the stress, because the history variables κ_1 and κ_2 are formulated in rate form in 7.

In the next part, the results of the modified rate-dependent damage model is presented. In this model, the rate factor is determined from the deformation rate in the element once damage has started. The

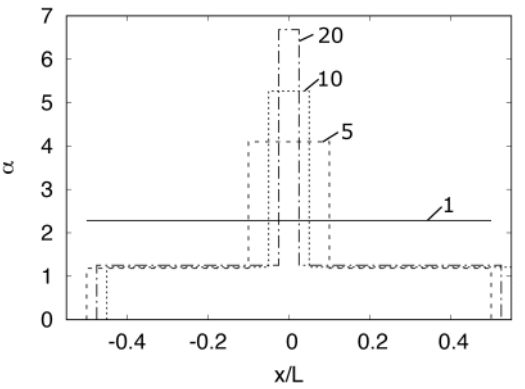

Figure 7. Rate factor versus x-coordinate for four meshes for the strain rate dependent damage model at a displacement of 0.1 mm.

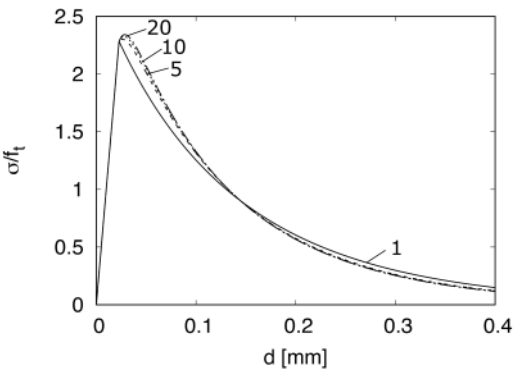

Figure 8. Load-displacement curves for four meshes for the deformation rate dependent damage model.

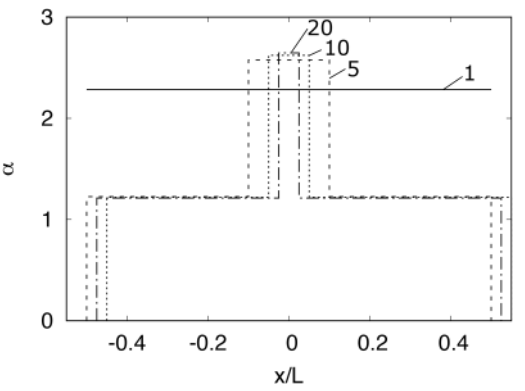

Figure 9. Rate factor profile for four meshes for the deformation rate dependent damage model at a displacement of 0.1 mm.

normalised stress versus displacement is shown in Figure 8. Furthermore, the rate factor versus the x-coordinate is shown in Figure 9. The normalised stress displacement curves are converging as the mesh is refined. Also, the rate factor in the damaged element converges with mesh refinement. Still, there is some

mesh dependence visible, because the rate factor in the damaged element is obtained from the total deformation rate in the element and not the crack opening rate. The crack band model describes crack openings mesh-independently, but not the deformation of the damaged element. Nevertheless, the finer the mesh, the smaller is the difference between deformation and crack opening rate.

4 CONCLUSIONS

We proposed a new approach to make a scalar damage model based on the crack band approach rate-dependent by switching at the onset of damage from a strain rate based to a deformation rate based formulation. It is shown that this formulation provides load-displacement curves which converge with mesh refinement. In the next step, the approach presented here will be applied to more comprehensive damage-plasticity models reported in (Grassl, Xenos, Nyström, Rempling, & Gylltoft 2013) and then used to investigate problems with wave propagation such as the spalling experiments reported in (Schuler, Mayrhofer, & Thoma 2006).

REFERENCES

Bažant, Z. P. & B.-H. Oh (1983). Crack band theory for fracture of concrete. *Materials and Structures 16*, 155–177.

Bischoff, P. H. & S. H. Perry (1991). Compressive behaviour of concrete at high strain rates. *Materials and structures 24*(6), 425–450.

CEB-FIP (2012). *CEB-FIP Model Code 2010, Design Code*.

Cusatis, G. (2011). Strain-rate effects on concrete behavior. *International Journal of Impact Engineering 38*, 162–170.

de Pedraza, V. R., F. Galvez, & D. C. Franco (2018). Measurement of fracture energy of concrete at high strain rates. In *EPJ Web of Conferences*, Volume 183, pp. 02065.

Doormaal, J. C. A. M. V., J. Weerheijm, & L. J. Sluys (1994). Experimental and numerical determination of the dynamic fracture energy of concrete. *Le Journal de Physique IV 4*(C8), C8–501.

Grassl, P., D. Xenos, U. Nyström, R. Rempling, & K. Gylltoft (2013). CDPM2: A damage-plasticity approach to modelling the failure of concrete. *International Journal of Solids and Structures 50*(24), 3805–3816.

Häussler-Combe, U. & T. Kühn (2012). Modeling of strain rate effects for concrete with viscoelasticity and retarded damage. *International Journal of Impact Engineering 50*, 17–28.

Malvar, L. J. & C. A. Ross (1998). Review of strain rate effects for concrete in tension. *ACI Materials Journal 95*, 735–739.

Patzák, B. (2012). OOFEM – An object-oriented simulation tool for advanced modeling of materials and structure. *Acta Polytechnica 52*, 59–66.

Piani, T. L., J. Weerheijm, & L. J. Sluys (2019). Dynamic simulations of traditional masonry materials at different loading rates using an enriched damage delay: Theory and practical applications. *Engineering Fracture Mechanics 218*, 106576.

Pietruszczak, S. T. & Z. Mróz (1981). Finite element analysis of deformation of strain-softening materials. *International Journal for Numerical Methods in Engineering 17*(3), 327–334.

Schuler, H., C. Mayrhofer, & K. Thoma (2006). Spall experiments for the measurement of the tensile strength and fracture energy of concrete at high strain rates. *International Journal of Impact Engineering 32*(10), 1635–1650.

Willam, K., N. Bićanić, & S. Sture (1986). Composite fracture model for strain-softening and localised failure of concrete. In E. Hinton and D. R. J. Owen (Eds.), *Computational Modelling of Reinforced Concrete Structures*, Swansea, pp. 122–153. Pineridge Press.